IOP Conf. Series: Materials Science and Engineering **1345** (2026) 012016 doi:10.1088/1757-899X/1345/1/012016

Integrated Platform for 2D Reel-to-Reel Characterization of 2G-HTS Superconductor Combining Raman Spectroscopy, Color Machine Vision, and Curvature Profiling

N. Castaneda[1*], C. Goel[1,3], D. Mayerich[2], G. Majkic[3]

[1] Materials Science and Engineering, University of Houston, Houston, TX 77024, USA
[2] Department of Electrical and Computer Engineering, University of Houston, Houston, TX, 77204, USA
[3] Department of Mechanical Engineering, University of Houston, Houston, TX 77204, USA, Texas Center for Superconductivity, University of Houston, Houston, TX 77004, USA, Advanced Manufacturing Institute, University of Houston, Houston, TX 77023, USA

[*]E-mail: ncastan4@cougarnet.uh.edu

Abstract. In this work, a two-dimensional (2D) reel-to-reel (R2R) platform integrating machine vision (MV), scanning Raman spectroscopy (SRS), and tape curvature profiling is presented for fast, non-destructive characterization of REBCO coated conductors (2G-HTS). The system enables rapid detection of defects, chemical variations, and curvature, as well as cross-comparison of the data to Scanning Hall Probe Microscopy (SHPM) measurements of critical current density (J_C). Operating at 10 m/h (MV) and 1.5 m/h (SRS), the platform enables high-speed scanning with M and selective rewinding for targeted, high-resolution SRS analysis of regions of interest (ROI). This integrated approach improves overall inspection efficiency and establishes fast, multi-modal scanning to complement conventional J_C-based quality control methods.

1. Introduction

The rapid advancement and broader implementation of second-generation high-temperature superconductors (2G-HTS), or REBCO coated conductors (CCs) (RE = Rare Earth (Y, Gd), Barium, Copper Oxide), across fusion energy, power transmission, and biomedical applications [1, 2], has intensified the need for robust quality control, characterization, and process monitoring. Large-scale projects, such as compact fusion reactors, require thousands of kilometers of REBCO tapes [3], emphasize the necessity for high-throughput, non-destructive metrology to ensure tape uniformity, critical current density (Jc) performance, and defect minimization.

Assessing Jc at application-relevant fields and temperatures (4.2–20 K, >5 T) remains challenging. While transport measurements and SHPM provide straightforward evaluation at 77 K, self-field (0 T) conditions, characterizing long lengths under high fields is complex [4]. Furthermore, localized or extended mild defects that suppress Jc are often difficult to detect by SHPM due to circulating current effects, underscoring the need for alternative approaches for fast, sensitive defect detection.

In response, our group has developed multiple reel-to-reel (R2R) inline and offline metrology platforms, including 2D X-ray diffraction (2D-XRD) integrated into the Advanced-Metal Organic

Content from this work may be used under the terms of the Creative Commons Attribution 4.0 licence. Any further distribution of this work must maintain attribution to the author(s) and the title of the work, journal citation and DOI.
Published under licence by IOP Publishing Ltd

Chemical Vapor Deposition (A-MOCVD) system, R2R SHPM for self-field and in-field Jc mapping, and in-field transport measurement systems for four-point I-V characterization at 65–77 K. These systems provide valuable insights into texture, strain, pinning efficiency, and in-field performance throughputs suitable for industrial production [5, 6].

To complement these efforts, we have explored Raman spectroscopy (RS) as a non-destructive technique capable of characterizing chemical composition, residual strain, oxygen content, and texture [7]. We have also investigated and demonstrated 2D Raman scanning capability (2D-SRS) along continuous tape lengths, successfully correlating Raman-derived material features with SHPM-detected defects and exploring relationships with in-field Jc performance [8]. Nevertheless, 2D-XRD and RS are constrained by scanning speeds: R2R 2D-XRD provides primarily linear maps (typically scans along the length of tape at the center across width), and for SRS the spatial resolution decreases with faster scanning to keep throughput at reasonable levels.

Building on these insights, we investigate machine vision (MV) as a complementary method for high-throughput 2D metrology. Despite its potential, MV remains underutilized for in-depth inspection and analysis of REBCO-coated conductors, with surprisingly few reports addressing its application in this context [9, 10]. Optimized imaging systems with controlled illumination can capture high-resolution 2D images (typically 12–50 mm in field of view) in fractions of a second, and scan speeds can be further increased through strobed lighting. Beyond shape-based analysis (e.g., defect detection), color imaging provides three channels of information that can be leveraged to infer film properties. Image analysis in hue, saturation, and brightness (HSV) or CIELAB 2000 color spaces enables quantification of subtle chemical and structural variations, with promising correlations to tape performance and critical current retention. Additionally, color-based analysis can aid in characterizing buffer layers. For instance, detecting slight thickness variations via hue shifts caused by thickness-dependent light interference in transparent multilayer films [11-13].

This work presents an integrated R2R platform integrating MV, scanning Raman spectroscopy, and tape height profiling for rapid, multi-modal characterization of REBCO tapes. The system simultaneously acquires spatially resolved Raman spectra, color images of the tape surface under controlled lighting, and curvature measurements. MV detects precipitates, localized defects, cracks, and chemical variations, while Raman mapping and independent SHPM scans provide chemical and magnetic Jc characterization. Tape profiling by focusing the Raman laser beam on the tape surface enables curvature analysis, which is in turn linked to residual strain and artificial pinning center (APC) density [14]. The system demonstrates reliable and repeatable performance, currently operating at scan rates of 10 m/h in MV mode and 1.5 m/h in SRS mode, with the possibility of selective tape rewinding for detailed high-resolution analysis of regions of interest identified via preliminary fast MV scans. In cases where higher Raman scanning speeds are needed, the system can operate in a line scan mode, sampling only the centerline of the tape, similar to inline XRD scanning [6]. The MV scan rate can be readily increased by at least an order of magnitude using synchronized strobe lighting.

2. Experimental

Segments of REBCO tape, 0.7 m and 4 m in length, were fabricated on $LaMnO_3$/Homo-Epi-MgO/IBAD-MgO/Al_2O_3/Hastelloy substrates using the A-MOCVD process. The tapes had a nominal composition of $Gd_{0.65}Y_{0.5}Ba_2Cu_3O_{7-x}$ + 0.05 Zr. Initial SHPM measurements, performed across the whole 12 mm tape width at a translation speed of 0.5 mm/s, revealed significant variations in the self-field Jc. Based on these findings, the 0.7 m segment was selected for detailed multi-modal characterization by SRS and MV in the integrated R2R system.

Raman scanning was performed using a Renishaw Virsa fibre-optic-coupled Raman analyzer equipped with a 532 nm laser operating at 25 mW. A 50 μm core optical fiber and a long working distance 50×/0.75 NA microscope objective were used, resulting in an approximate laser spot size of ~6 μm. The spectrometer provides a spectral dispersion of <1.5 cm−1/pixel and a spectral resolution of <2.5 cm−1, with a thermoelectrically cooled detector array of 1024 × 256 pixels. The spectral acquisition range spans from 50 cm−1 to 4000 cm−1. LiveTrack™ focus tracking technology was employed to maintain continuous focus on the sample during both measurement and visualization.

For fast Raman measurements, the REBCO tape segments were scanned in reel-to-reel (R2R) mode at a translation speed of 0.5 mm/s and a zigzag Raman scanning pattern consisting of 54 points per diagonal and an integration time of 0.5 s per point. The Raman mapping template can be readily modified and adapted to meet specific scanning requirements. Raw Raman spectra were postprocessed using a custom-made code that includes cosmic ray and outlier removal, background subtraction, and Voigt peak fitting [7]. Characteristic wavenumbers and integrated intensities of selected peaks were extracted from these fits.

For two-dimensional (2D) imaging by machine vision (MV), a telecentric lens with a working distance of 163.5 mm, paired with a 1.1” sensor offering a horizontal field of view of 48.02 mm and a total imaging area of 38.4 × 28.8 mm2 (H × V), was connected to a color camera featuring a 1.1” progressive scan CMOS sensor (4096 × 3000 pixels) with GigE (PoE) output. Illumination was provided by a flat dome white LED light source (143 × 143 × 13.1 mm^3), equipped with a dot-patterned diffusion plate to ensure uniform light distribution across the tape surface. Image acquisition was performed at an R2R speed of 10 mm/s with a 7 ms exposure time.

Postprocessing of the MV data was performed using a custom MATLAB code for image correction and segmentation. Flat field correction was applied before stitching to ensure image consistency and remove spatial illumination non-uniformities. The corrected and stitched images were then converted into the HSV (Hue, Saturation, Value) color space to analyze surface color variations, particularly through the hue channel, representing color type as an angle on a color wheel. To quantify local hue uniformity, we extracted eccentricity values from the angular distribution of hue, a metric further interpreted in the Results section as an indicator of surface deposition quality and defect presence.

3. Results

3.1 Machine Vision Color Segmentation

Figure 1 shows the results of the Machine Vision (MV) imaging implemented in the R2R system for surface analysis of a 0.7-meter-long, 12 mm-wide REBCO tape. The stitched RGB image (Figure 1a) reveals surface inhomogeneities, with the left half of the tape exhibiting greater textural variation than the more uniform right half.

Images were converted into the HSV (Hue, Saturation, Value) color space to analyze these variations. In this model, hue (Figure 1b) represents the color tone as an angle in polar coordinates (on the color wheel (0–360°), saturation (Figure 1c) indicates color purity, and value (Figure 1d) corresponds to brightness. Variations across these three components expose subtle but meaningful changes in surface appearance that hint at underlying material changes ranging from composition variation to damage.

We introduced a metric to quantify hue distribution: the eccentricity of the hue angle distribution (Figure 2a). For each longitudinal position along the tape (X), eccentricity is computed by fitting the hue values of this local X region obtained across the tape width to an ellipse in polar coordinates. Values approaching 1 indicate a narrow, directional hue distribution (signifying uniform surface deposition),

whereas values near 0 suggest dispersed hue distributions indicative of non-uniform deposition or localized defects.

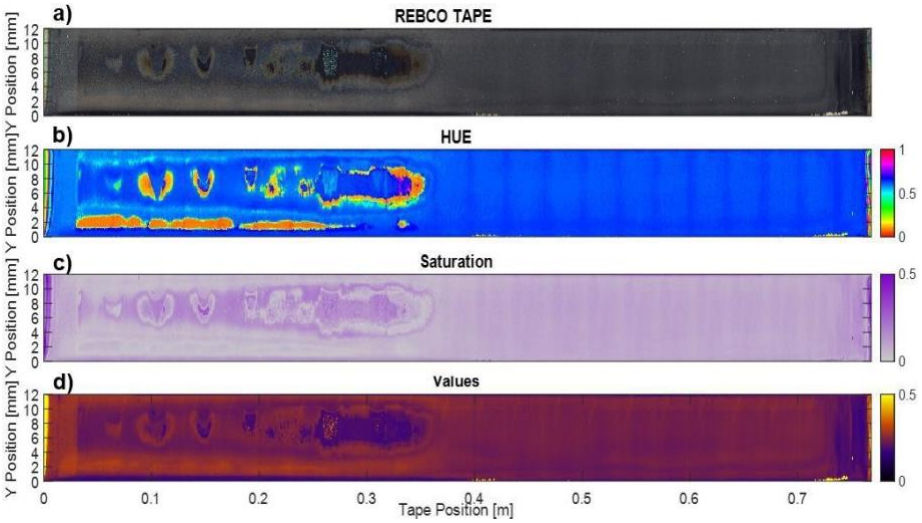

Figure 1. Surface analysis via machine vision. (a) Stitched RGB image. (b–d) HSV-segmented images showing hue, saturation, and value distributions, respectively.

Figure 2b displays the longitudinal eccentricity profile along the tape. Notably, two visually consistent regions (red squares 1 and 2) exhibit sudden drops in eccentricity. As highlighted in Figure 2c, these correspond to edge-related defects, such as tape delamination or peel-off, underscoring the sensitivity of eccentricity as a surface quality metric. Figure 2d shows polar histograms of hue angles from selected tape regions. Uniform areas exhibit tightly grouped hue angles (210°–240°), while defective areas show broader angular distributions.

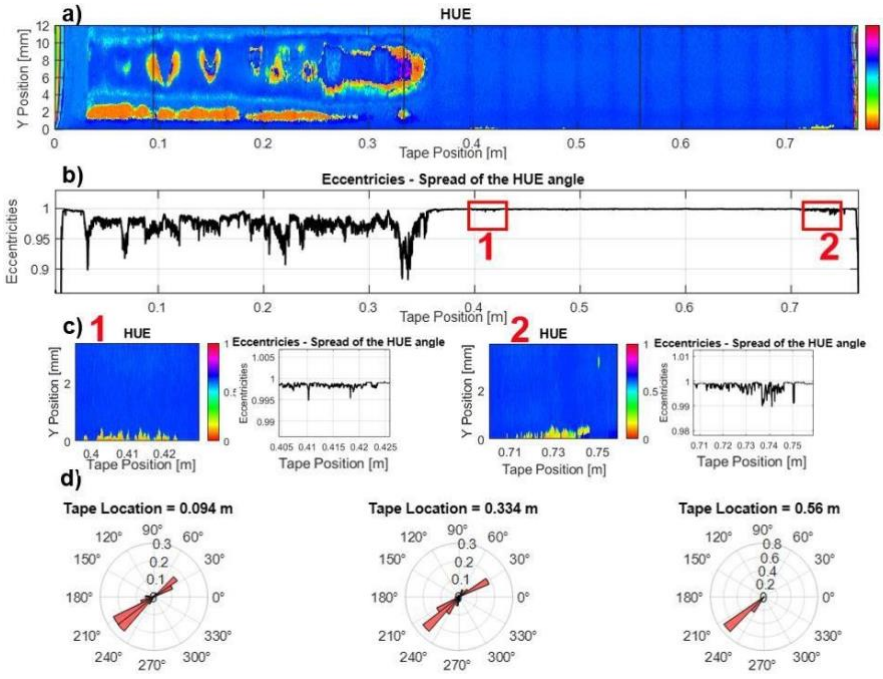

Figure 2. Eccentricity analysis of hue distribution. (a) Hue-segmented image. (b) Longitudinal eccentricity profile highlighting regions 1 and 2. (c) Magnified views of regions with local eccentricity drops. (d) Polar histograms of hue angle distributions from selected tape regions.

This approach demonstrates that eccentricity in HSV hue space offers a sensitive metric for surface uniformity and defect detection, with potential for utilizing it even for real-time feedback during tape deposition.

3.2 Cross-Comparison SHPM I_c, Hue, and Raman 2D Maps

Figure 3 shows the cross-comparison of 2D maps obtained from SHPM, MV hue segmentation, and Raman spectroscopy. In the SHPM critical current map (Figure 3a), the zero I*c* region ('line') along the middle of the tape width is an artifact due to magnetization (change in direction of the circulating current loop). However, a distinct critical current drop is observed in the entire first half of the tape, with near-zero values and in the area marked by a black square.

Figure 3b, the hue-segmented image, highlights the same degraded region identified in the SHPM map, with sharp eccentricity fluctuations further confirming the presence of non-uniform surface features. Raman mapping (Figure 3 c–e) provides further insight: the c-axis grain (O2/O3-) peak intensity, the shift in oxygen content (O4) peak wavelength, and a-axis grain (O4) peak intensity all point to a structural breakdown in the REBCO layer, particularly on the left side of the tape. Although peak intensity of O2/O3- remains detectable, the wavelength shift in the O4 peak suggests poor oxygenation and altered composition [15, 16]. Additionally, wavelength shifts in other characteristic peaks (e.g., Cu, Ba and O2/O3+) indicate a strong presence of the tetragonal phase, which helps explain the significant loss of superconducting performance in this region [17, 18].

Collectively, the MV and Raman data validate the SHPM results and reveal that the left portion of the tape is structurally compromised. This multi-modal alignment confirms the utility of integrating MV and SRS for rapid, informative quality control.

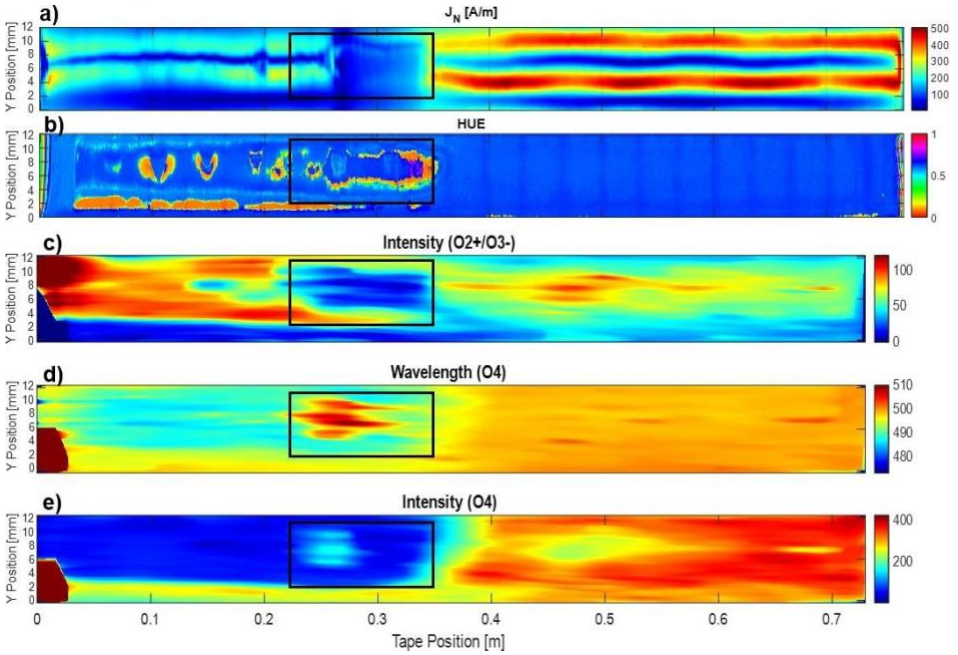

Figure 3. Comparative 2D maps of the same REBCO tape. (a) SHPM J*c* map. (b) Hue-segmented MV image. (c–e) Raman maps showing c-axis grain peak intensity, O4 peak wavelength (oxygen content), and a-axis grain peak wavelength, respectively.

3.3 High-Resolution Raman Analysis of Defective Region

To explore the degradation further, detailed Raman scans were performed in the affected region. The following scans were done sequentially after initial fast MV scan from which the defective regions were

identified. Figure 4a shows the area identified via hue segmentation; Figure 4b provides the corresponding optical microscopy image, which clearly displays surface cracking and delamination.

Raman mapping of this zone (Figure 4c) reveals two unexpected peaks: one at ~650 cm-1, characteristic of the buffer layer, and another at ~1560 cm-1, which may relate to contamination, The presence of buffer layer signal suggests that the REBCO film has been breached, exposing underlying layers. These observations confirm severe surface and structural damage in the affected area and demonstrate how MV can be used to flag defects for targeted Raman inspection.

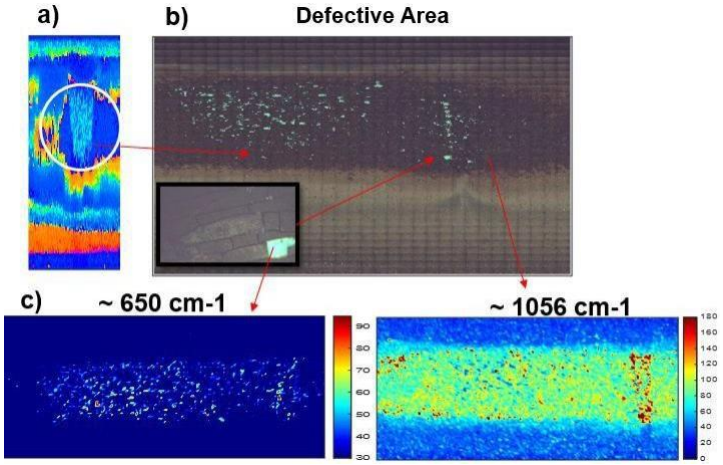

Figure 4. High-resolution characterization of a defective region. (a) Hue-segmented identification of the region. (b) Optical micrograph showing cracking and peel-off. (c) Raman maps of non-REBCO peaks, indicating exposure of the buffer layer and altered chemical composition.

3.4 Curvature Profiling and Raman Strain Mapping

The R2R system also integrates autofocus technology at each point during Raman scanning, which can be used for curvature profiling. This, combined with Raman analysis of the O2/O3- peak position, enables non-contact strain mapping [19]. Since curvature is directly linked to strain, this integration provides a unique way to monitor strain due to the introduction of nanorods in REBCO tapes.

Figure 5b displays a 3D curvature map of a 100 μm section of 12 mm-wide tape done sequentially after MV scans, showing clear surface profile variation that correlates with Raman-detected strain areas. The shift of O2/O3- wavelength is indicative of local strain in REBCO [19]. The figure shows the curvature profile measured by laser focusing, as well as O2/O3- wavelength. In the area marked with red rectangles, the increase in local curvature and thus strain matches with a shift in O2/O3- towards lower wavenumbers. However, on the opposite end of the tape, curvature again increases compared to the tape center, but O2/O3- wavenumber does not shift compared to the middle section. Although, further inspection of the tape revealed an array of dense scratches in the REBCO layer propagating along the length of the tape, as can also be seen in Figure 5c. It suggests that the curvature in this region is imparted to the tape via plastic deformation evident from scratches, thus leaving the REBCO layer at low strain. This particular region of interest reveals the possibility of combining strain information from O2/O3- shift and curvature profiling to obtain a more complete picture of local strain states than either technique alone. In addition, as introduction of artificial pinning centers (APCs), in particular nanorods in the form of $BaMO_3$ (where M=Zr, Hf, Sn [14, 20]), introduces residual mismatch strain in the REBCO matrix, the strain mapping can be potentially used as an indirect measure of local density of APCs. Furthermore, combined curvature profile and O2/O3- wavelength maps can provide a way of

distinguishing between strain in REBCO film and tape deformation/damage, e.g., due to conveyance issues during deposition.

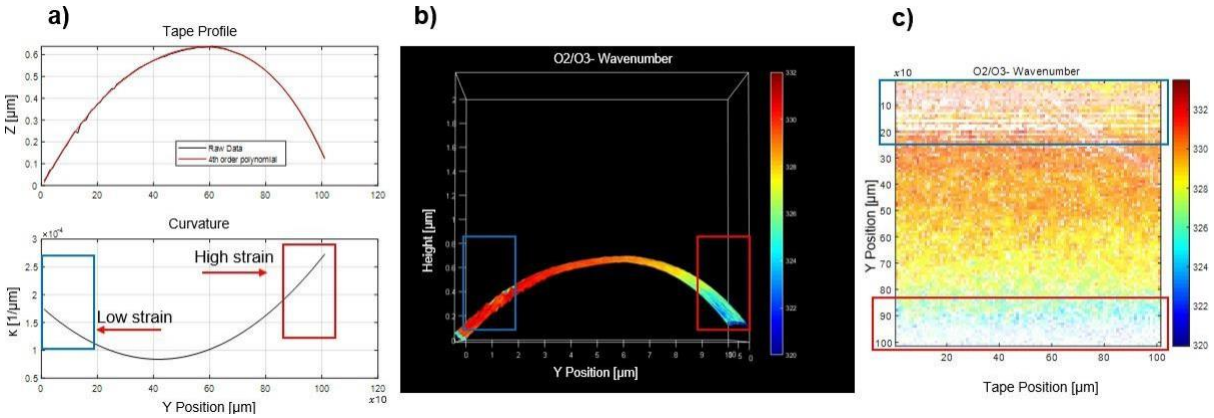

Figure 5. (a) Schematic of curvature-strain relationship. (b) The 3D curvature map derived from autofocus scanning shows strain distribution across the tape width.

4. Summary

This study reports on the development of an integrated platform for R2R characterization of 2G-HTS conductors integrating 2D Raman Spectroscopy, color Machine Vision and tape curvature profiling. The system currently operates at 10 and 1.5 m/hr in MV and Raman scanning modes, respectively. The transformation of MV color maps into the HSV color space enabled segmentation of tape nonuniformities and defective regions, with the potential for further correlation of individual H, S, and V components with tape I*c* performance. Raman scans of O2/O3-, O4 intensity, and O4 wavenumber revealed correlation with I*c* maps obtained from SHPM, including not only identification of a defective region but also changes in I*c* performance along the tape in defect-free regions, as well as low I*c* regions near the tape edge. The tape curvature profiling was demonstrated to provide high-resolution 2D curvature profiles of tape, which can be utilized as an indirect measure of local density of artificial pinning centers such as $BaMO_3$ nanorods.

Acknowledgments
This work was funded by Advanced Manufacturing Institute (AMI) – University of Houston.

References

[1] W. H. Fietz, C. Barth, S. Drotziger, W. Goldacker, R. Heller, S. I. Schlachter, and K.-P. Weiss, "Prospects of High Temperature Superconductors for fusion magnets and power applications," *Fusion Engineering and Design,* vol. 88, no. 6-8, pp. 440-445, 2013.

[2] A. Molodyk, and D. C. Larbalestier, "The prospects of high-temperature superconductors," *Science,* vol. 380, no. 6651, pp. 1220-1222, Jun 23, 2023.

[3] A. Molodyk, S. Samoilenkov, A. Markelov, P. Degtyarenko, S. Lee, V. Petrykin, M. Gaifullin, A. Mankevich, A. Vavilov, B. Sorbom, J. Cheng, S. Garberg, L. Kesler, Z. Hartwig, S. Gavrilkin, A. Tsvetkov, T. Okada, S. Awaji, D. Abraimov, A. Francis, G. Bradford, D. Larbalestier, C. Senatore, M. Bonura, A. E. Pantoja, S. C. Wimbush, N. M. Strickland, and A. Vasiliev, "Development and large volume production of extremely high current density YBa2Cu3O7 superconducting wires for fusion," *Sci Rep,* vol. 11, no. 1, pp. 2084, Jan 22, 2021.

[4] X. F. Li, A. B. Yahia, G. Majkic, M. Kochat, S. Kar, and V. Selvamanickam, "Reel-to-reel critical current measurement of REBCO coated conductors," *IEEE Transactions on Applied Superconductivity,* vol. 27, no. 4, pp. 4-8, 2017.
[5] S. Chen, X.-F. Li, W. Luo, and V. Selvamanickam, "Reel-to-Reel Scanning Hall Probe Microscope Measurement on REBCO Tapes," *IEEE Transactions on Applied Superconductivity,* vol. 29, no. 5, pp. 1-4, 2019.
[6] S. Chen, G. Majkic, R. Jain, R. Pratap, V. Mohan, C. Goel, and V. Selvamanickam, "Scale Up of High-Performance REBCO Tapes in a Pilot-Scale Advanced MOCVD Tool With In-Line 2D-XRD System," *IEEE Transactions on Applied Superconductivity,* vol. 31, no. 5, pp. 1-5, 2021.
[7] N. Castaneda, G. Majkic, and F. C. Robles, "Scanning Raman spectroscopy for inline characterization of 2G-HTS conductors," *Superconductor Science and Technology,* vol. 34, no. 3, 2021.
[8] N. Castaneda, C. Goel, G. Majkic, F. Robles, and V. Selvamanickam, "Scanning Raman Spectroscopy Characterization of 1 Meter Long REBCO Coated Conductor.," *IOP Conf. Series: Materials Science and Engineering,* vol. 1302 012012, 2024.
[9] J. Zhu, M. Tong, S. Chen, Y. Zhao, C. Lou, Z. Zhang, Z. Gao, B. Song, W. Zhu, J. Sheng, Z. Zhang, and Z. Jin, "Online perception on the performance of YBCO tapes via intelligent video-aided PLD system," *Physica C: Superconductivity and its Applications,* vol. 598, pp. 1354066, 2022.
[10] J.-H. Lee, M. Byoung-Jean, K. Tae-Jin, K. Young-Soon, C. Kyekun, K. Taehoon, P. Dae-Gwan, S. Dae-Won, K. Ho-Kyum, C. Woosuk, L. Hunju, and M. Seung-Hyun, "Vision Inspection Methods for Uniformity Enhancement in Long-Length 2G HTS Wire Production," *IEEE Transactions on Applied Superconductivity,* vol. 24, no. 5, pp. 1-5, 2014.
[11] J. Beyerer, F. León, and C. Frese, *Machine Vision: Automated Visual Inspection: Theory, Practice and Applications*, 2015.
[12] C. Steger, M. Ulrich, and C. Wiedemann, *Machine vision algorithms and applications*: John Wiley & Sons, 2018.
[13] A. Hornberg, *Handbook of machine vision*: John Wiley & Sons, 2006.
[14] G. Majkic, J. S. Jeong, H. Yun, F. C. Robles Hernandez, E. Galstyan, R. Pratap, H. Cheng, A. Stokes, K. A. Mkhoyan, and V. Selvamanickam, "New insight into strain and composition of BaZrO3 nanorods in REBCO superconductor," *Superconductor Science and Technology,* vol. 34, no. 11, pp. 115002, 2021/09/28, 2021.
[15] C. Camerlingo, I. Delfino, and M. Lepore, "Micro-Raman spectroscopy on YBCO films during heat treatment," *Superconductor Science and Technology,* vol. 15, no. 11, pp. 1606-1609, 2002.
[16] M. N. Iliev, P. X. Zhang, H. U. Habermeier, and M. Cardona, "Raman spectroscopy as analytical tool for the local structure of YBa2Cu3Ox thin films," *Journal of Alloys and Compounds,* vol. 251, no. 1-2, pp. 99-102, 1997.
[17] M. N. Iliev, "Raman Spectroscopy of Phase Separation and Reordering Processes in YBCO-Type Compounds," *ACS Symposium Series; American Chemical Society*, pp. 107-119, 1999.
[18] K. Lange, M. Sparkes, J. Bulmer, J. Feighan, W. O'Neill, and T. Haugan, "Analysing laser machined YBCO microbridges using raman spectroscopy and transport measurements aiming to investigate process induced degradation," *Lasers in Engineering,* vol. 46, 2020.
[19] L. Zeng, Y. M. Lu, Z. Y. Liu, C. Z. Chen, B. Gao, and C. B. Cai, "Surface texture and interior residual stress variation induced by thickness of YBa 2Cu 3O 7-δ thin films," *Journal of Applied Physics,* vol. 112, no. 5, 2012.
[20] C. Cantoni, Y. Gao, S. H. Wee, E. D. Specht, J. Gazquez, J. Meng, S. J. Pennycook, and A. Goyal, "Strain-Driven Oxygen Deficiency in Self-Assembled, Nanostructured, Composite Oxide Films," *ACS Nano,* vol. 5, no. 6, 2011/06/28, 2011.